Twelfth Australasian Fluid Mechanics Conference
The University of Sydney, Australia 1995

EFFECT OF RATE OF INCREASE OF THE INNER CYLINDER SPEED ON SELECTION OF THE FINAL WAVELENGTH IN TAYLOR VORTEX FLOW

John Rigopoulos, Mark C. Thompson and John Sheridan
Department of Mechanical Engineering
Monash University
Clayton, Victoria
AUSTRALIA

ABSTRACT

A spectral numerical method was used to model linear increases in inner cylinder Reynolds number during a finite ramp time for Taylor vortex flow. The outer cylinder was kept stationary. The annulus was of infinite height and modelled using periodic boundary conditions. The final Reynolds number was restricted to a region close to the critical Reynolds number for the onset of Taylor vortex flow. How different ramp times affects the growth in the amplitude of the modes with time and the selection of the axial wavelength at steady state was investigated. Longer ramp times resulted in the amplitudes of the unpreferred modes becoming less significant in comparison with the amplitude of the preferred mode. For almost sudden increases in Reynolds number there was an interplay between the different modes before one eventually dominated in the development of the flow.

INTRODUCTION

Taylor vortex flow can develop in a fluid bounded by two concentric rotating vertical cylinders. The flow is axisymmetric, an example of which is shown in Figure 3. An experimental investigation was undertaken by Burkhalter and Koschmieder (1973), (1974) for quasi-steady and sudden increases in inner cylinder Reynolds number, respectively. The authors' results indicated that for a sudden increase in inner cylinder Reynolds number (Re_{in}) to a value above but close to the critical Reynolds number for the onset of Taylor vortices (Re_c), the selected wavelength (λ_s) was generally less than the critical wavelength (the wavelength λ_c derived from linear theory) and varied as shown in Figure 1. However, it was found that λ_s equaled λ_c for quasi-steady increases in Re_{in}. A numerical investigation by Neitzel (1984) was conducted for finite height annuli, rigid endwalls attached to and moving with the inner cylinder, and sudden starts. The author's results showed close agreement with the selected wavelengths determined by Burkhalter and Koschmieder (1974) in a Reynolds number region close to the critical value for the onset of Taylor vortices.

METHOD

The axisymmetric, incompressible Navier-Stokes equation in cylindrical coordinates were solved numerically using a Fourier-Chebyshev Spectral method and with the use of operator splitting. We defined Reynolds number in the same manner as Marcus (1984). A Fourier approximation was made in the axial direction with M points and a Chebyshev approximation was made in the radial direction with N points. All derivatives were determined using a Fourier-Chebyshev derivative transform routine. The non-linear (convection) step used a second-order Adams-Bashforth approximation, an explicit scheme. The velocity in the second fractional step was adjusted to make it divergence free. The pressure was solved from a Poisson equation obtained by enforcing the incompressibility constraint on the velocity at the second fractional step. First-order Neumann pressure boundary conditions were used, as described by Karniadakis *et al.* (1991). The viscous step used an implicit approximation incorporating a weighting factor θ. For example, $\theta = 0$ corresponded to a Crank-Nicholson approximation and $\theta = 0.5$ corresponded to a Backward-Euler approximation. The viscous step reduced to a Helmholtz equation for the velocity. Both the Poisson and Helmholtz solvers were based on a Fourier-Chebyshev Spectral Tau method. In the Tau method the equation is solved in spectral space first for the coefficients and then backtransformed to

real space to get the pressure and velocity component distributions. The Poisson equation and the Helmholtz equation were arranged to have factors r and r^2 in front of the derivative terms. In spectral space these factors had easily-derivable arrays which were multiplied with the spectral form of the derivative terms. The $3M$ inversions of $(N-2)\times(N-2)$ arrays needed only to be done once, in a pre-processing step.

The code was checked for accuracy by comparing the growth rates in the initial stage of exponential growth of the vortices with results from other sources. Results are shown in Table 1. The initial conditions were circular Couette flow plus a small random perturbation. The referenced results in cases 1 and 3 come from Marcus (1984) and case 2 is from linear theory. As can be seen, our growth rates agree to at least three decimal places for the chosen numerical parameters.

CASE	1	2	3
η	0.5	0.5	0.95
μ	0	0.11765	0
Re_{in}	74.924	82.557	184.99
Γ	1.9877	2.0268	2.0087
Δt	0.05	0.05	0.5
$M \times N$	16×17	16×17	16×17
θ	0	0.5	0.1
Computed	0.035649	0.000106	0.000003
Referenced	0.035636	0.0	0.000516

TABLE 1: Comparison of growth rates. Radius ratio (inner/outer) η, angular velocity ratio (outer/inner) μ, aspect ratio (height of annulus) Γ.

In our numerical simulations the Reynolds number (Re) was increased linearly with time from an initial Re_i to a final Re_f over a ramp time T, and then the simulation was continued until steady state at the value of Re_f.

A high aspect ratio confirmation of this method can be seen from the case $\eta = 0.5$, $\mu = 0$, $Re_f = 74.924$, $Re_i = 60$, $\Gamma = 19.877$ with $\Delta t = 0.25$, $M = 324$, $N = 33$, $\theta = 0$, and $T = 40$ revs (very slow increases of Re). This gave the result $\lambda_s = 1.9877$. In other words, the selected wavelength in this case is the critical wavelength, as expected for quasi-steady ramps.

A variation of Re would normally require $2M$ of the $3M$ matrix inversions described above to be done at every time step. This would make the spectral method too computationally time consuming. To overcome this a variable time spacing was used while Re was varied so that the ratio $Re/\Delta t$ remained constant. Then these $2M$ inversions were only needed to be done once, as for the constant-Re situation.

RESULTS

The following choice of parameter values were made: $\eta = 0.727$, $\mu = 0$, $Re_f = 116.67$, $Re_i = 70$, and aspect ratio $\Gamma = 20.0286$. These values were selected so a comparison of the results of Burkhalter and Koschmieder (1974) and Neitzel (1984) could be made with selected wavelength. The numerical parameters were set to $\Delta t = 0.25$, $M = 324$, $N = 33$ and $\theta = 0$. These values were decided upon after a long series of runs where resolution requirements in space and time were determined, for the case of ramp time $T = 2.98826$ revs (inner cylinder revolutions). Comparisons of maximum and minimum azimuthal vorticity and the distance between successive extrema for different selections of the numerical parameters were made to check that the same final state was reached.

To investigate the effect of the rate of increase of the inner cylinder speed on the computed wavelength the steady state wavelengths were computed for different ramp times. A plot of computed wavelength versus ramp time is shown in Figure 2 together with points from Burkhalter and Koschmieder (1974), and Neitzel (1984).

In Figure 3 we show a velocity vector plot for the state $\lambda_s = 1.821$.

For different ramp times, the spectral amplitude for each mode was studied at different times during the development of the flow. Examples of these are shown in Figure 4. The spectral amplitude $A_m(t)$, where m specifies the axial mode, was taken as the Fourier transform of the radial component of velocity at the radial centre of the domain.

DISCUSSION

We compared our results with Burkhalter and Koschmieder (1974) and Neitzel (1984) for selected wavelength for sudden starts ($T = 0$) and quasi-steady increases (T sufficiently large). For $T \leq 0.0095$ revs we obtained $\lambda_s = 1.669$ and for $0.00955 \leq T \leq 29.8826$ revs we obtained $\lambda_s = 1.821$. This compared with $\lambda_s = 1.75$ for sudden starts and $\lambda_s = 2.0$ for quasi-steady increases, by the two authors. Our results were reasonable given that in the vicinity of the selected wavelengths only axial wavelengths of 1.541, 1.669, 1.821 and 2.003 could be selected. Also, the experimental results were restricted to discrete values and had end conditions which were different to ours.

Hence, Figure 2 indicates that the preferred wavelength remains at the value 1.821 until Re increases in an almost stepwise fashion. Then the preferred wavelength drops to the value 1.669 .

Figure 4 shows that although the jump from the wavelengths 1.821 to 1.669 occurs for a particular value of ramp time, the spectral amplitudes reveal that for a decreased ramp time the unpreferred modes become more significant in a continuous manner. In particular, as the ramp time is decreased, the amplitude of the 1.669 mode rises and concurrently the amplitude of the 1.821 mode drops, after the initial ex-

ponential growth region, as shown in Figures 4.1 and 4.2 . Eventually a steep enough ramp will make the 1.669 mode overtake and dominate the 1.821 mode, as shown in Figure 4.3 . The 1.669 mode will grow to a finite amplitude and the 1.821 will decay to zero.

Figure 4.2 highlights an intermediate situation where the 1.669 mode overtakes the 1.821 mode but the ramp time is short enough to keep the 1.669 mode from eventually decaying to zero again, with the 1.821 mode eventually dominating.

Figure 4.3 also indicates for sudden starts that although the amplitude of the 1.821 mode is greater than the amplitude of the 1.669 mode in the initial region of exponential growth, there is a time during the development of the flow where the 1.669 mode overtakes the 1.821 mode and becomes the selected mode at steady state.

CONCLUSION

It has been shown by fixing the initial and final Reynolds number and varying the speed of the ramp between them that the selected wavelength at steady state is affected by the rate of increase of the inner cylinder speed. The fastest growing mode in the initial stage of exponential growth doesn't always dominate in the development of the flow and isn't always the selected mode at steady state. For faster increases in Re_{in} the amplitudes of the unpreferred modes become more significant in comparison with the preferred mode. When a short enough ramp time is applied there is interplay between the modes before one mode eventually dominates. The next stage of this research will look at higher aspect ratio values and focus on an understanding of the physical process behind wavelength selection from a linear rate of increase of inner cylinder speed.

REFERENCES

Burkhalter, J. E. and Koschmieder, E. L., 1973, "Steady supercritical Taylor vortex flow", Journal of Fluid Mechanics, Vol. 58, p.p. 547-560.

Burkhalter, J. E. and Koschmieder, E. L., 1974, "Steady supercritical Taylor vortices after sudden starts", Physics of Fluids, Vol. 17, p.p. 1929-1935.

Karniadakis, G. E., Israeli M., and Orszag S. A., 1991, "High-order splitting methods for incompressible Navier-Stokes equations", Journal of Computational Physics, Vol. 97, p.p. 414-443.

Marcus, P. S., 1984,"Simulation of Taylor-Couette flow. Part 1. Numerical methods and comparison with experiment", Journal of Fluid Mechanics, Vol. 146, p.p. 45-64.

Neitzel, G. P., 1984, "Numerical computation of time-dependent Taylor-vortex flows in finite-length geometries", Journal of Fluid Mechanics, Vol. 141, p.p. 51-66.

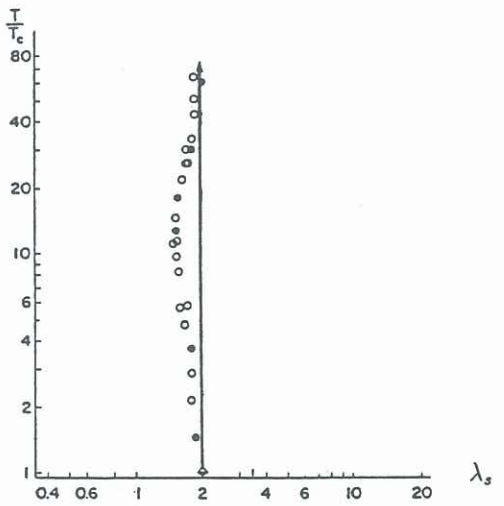

FIGURE 1: Ratio of Taylor number to critical Taylor number versus selected wavelength for $\eta = 0.727$, $\mu = 0$. Data from Burkhalter and Koschmieder (1974). The circled points are for sudden starts. The vertically straight line is for quasi-steady increases.

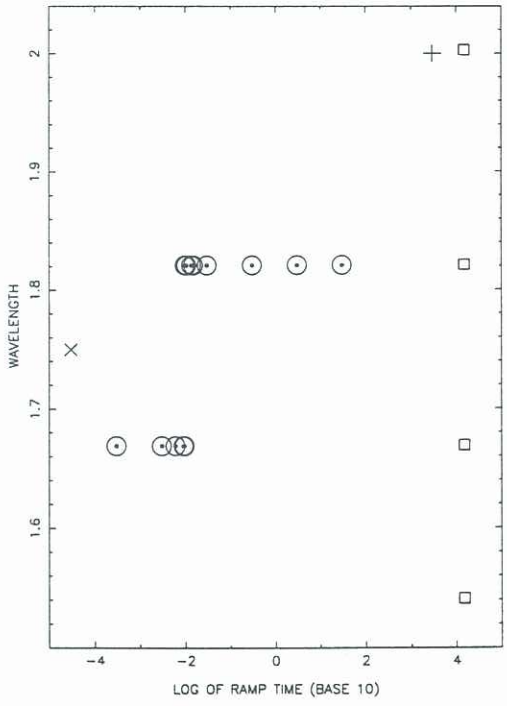

FIGURE 2: Selected wavelength versus ramp time. Time in units of inner cylinder revolutions. Our numerical experiments (⊙).The discrete possible wavelengths in our numerical experiments in the vicinity of the selected wavelengths (□). Burkhalter and Koschmieder (1974), Neitzel (1984) (×). Burkhalter and Koschmieder (1974) (+).

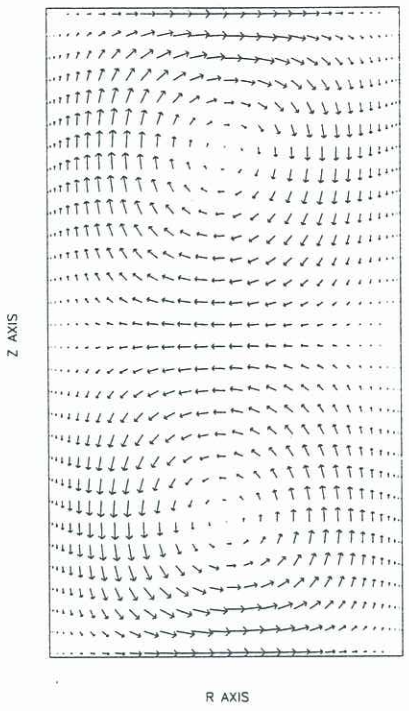

FIGURE 3: Velocity vector plot of the $\lambda_s = 1.821$ mode.

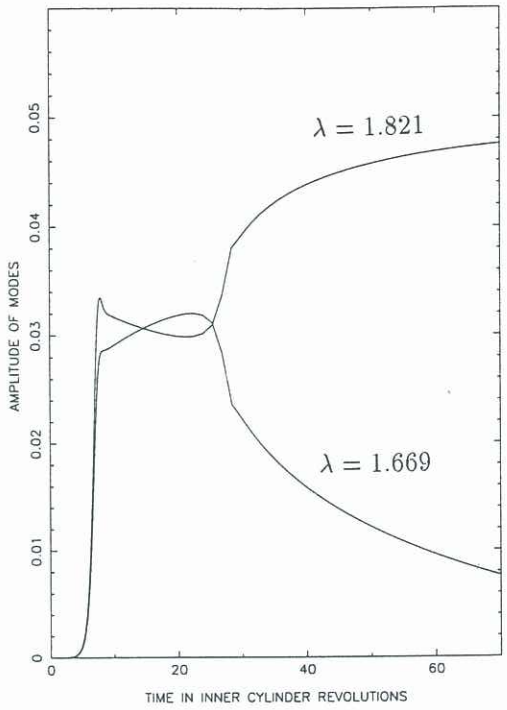

FIGURE 4.2: A_m versus time for ramp time $T = 0.00955$ revs.

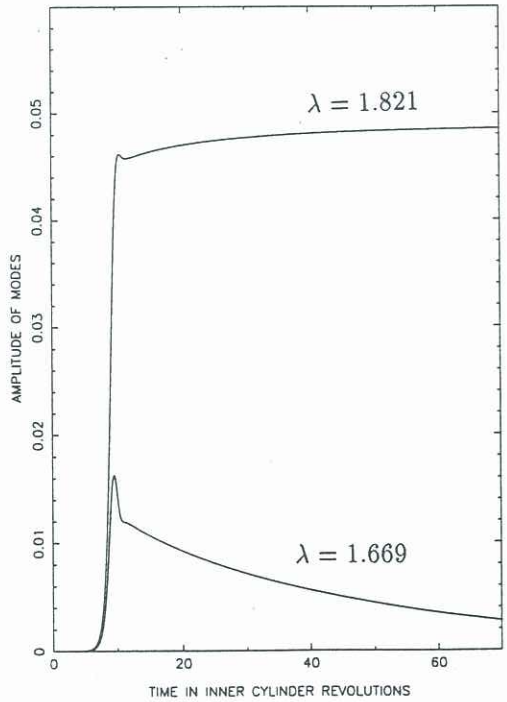

FIGURE 4.1: A_m versus time for ramp time $T = 2.98826$ revs.

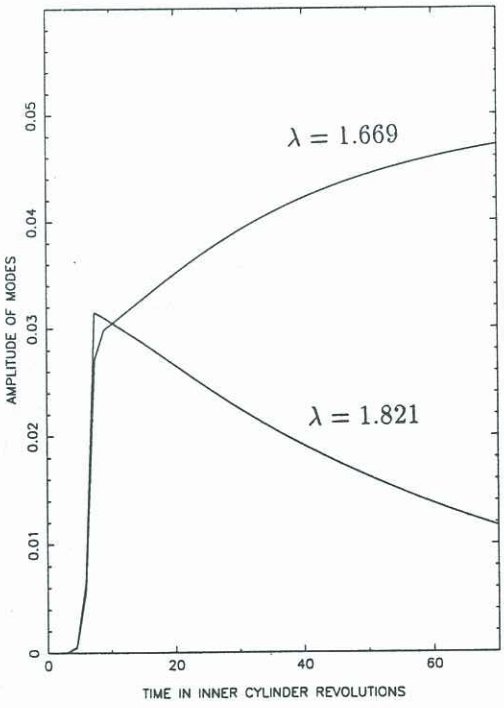

FIGURE 4.3: A_m versus time for ramp time $T = 0$ revs.